Journal of *Personalized Medicine*

MDPI

*Article*

# Potential Role of miRNAs in the Acquisition of Chemoresistance in Neuroblastoma

**Barbara Marengo [1,*,†], Alessandra Pulliero [2,†], Maria Valeria Corrias [3,†], Riccardo Leardi [4], Emanuele Farinini [4], Gilberto Fronza [5], Paola Menichini [5], Paola Monti [5], Lorenzo Monteleone [1], Giulia Elda Valenti [1], Andrea Speciale [5], Patrizia Perri [3], Francesca Madia [6], Alberto Izzotti [1,5,†] and Cinzia Domenicotti [1,†]**

1 Department of Experimental Medicine, University of Genova, 16100 Genova, Italy; lolloleo92@gmail.com (L.M.); giuliaelda.valenti@edu.unige.it (G.E.V.); alberto.izzotti@unige.it (A.I.); cinzia.domenicotti@unige.it (C.D.)
2 Department of Health Sciences, University of Genova, 16100 Genova, Italy; alessandra.pulliero@unige.it
3 Laboratory of Experimental Therapies in Oncology, IRCCS Istituto Giannina Gaslini, 16100 Genova, Italy; mariavaleriacorrias@gaslini.org (M.V.C.); patriziaperri@gaslini.org (P.P.)
4 Department of Pharmacy, University of Genova, 16100 Genova, Italy; riclea@difar.unige.it (R.L.); farinini@difar.unige.it (E.F.)
5 UOC Mutagenesis and Cancer Prevention, IRCCS Ospedale Policlinico San Martino, 16100 Genova, Italy; gilberto.fronza@hsanmartino.it (G.F.); paola.menichini@hsanmartino.it (P.M.); paola.monti@hsanmartino.it (P.M.); andreaspeciale@alice.it (A.S.)
6 Medical Genetics Unit, IRCCS Giannina Gaslini Institute, 16100 Genova, Italy; francescamadia@gaslini.org
* Correspondence: barbara.marengo@unige.it; Tel.: +39-010-3538831
† These authors contributed equally to this work.

**Abstract:** Neuroblastoma (NB) accounts for about 8–10% of pediatric cancers, and the main causes of death are the presence of metastases and the acquisition of chemoresistance. Metastatic NB is characterized by *MYCN* amplification that correlates with changes in the expression of miRNAs, which are small non-coding RNA sequences, playing a crucial role in NB development and chemoresistance. In the present study, miRNA expression was analyzed in two human *MYCN*-amplified NB cell lines, one sensitive (HTLA-230) and one resistant to Etoposide (ER-HTLA), by microarray and RT-qPCR techniques. These analyses showed that miRNA-15a, -16-1, -19b, -218, and -338 were down-regulated in ER-HTLA cells. In order to validate the presence of this down-regulation in vivo, the expression of these miRNAs was analyzed in primary tumors, metastases, and bone marrow of therapy responder and non-responder pediatric patients. Principal component analysis data showed that the expression of miRNA-19b, -218, and -338 influenced metastases, and that the expression levels of all miRNAs analyzed were higher in therapy responders in respect to non-responders. Collectively, these findings suggest that these miRNAs might be involved in the regulation of the drug response, and could be employed for therapeutic purposes.

**Keywords:** neuroblastoma; miRNA; *MYCN* amplification; metastases; chemoresistance



**Citation:** Marengo, B.; Pulliero, A.; Corrias, M.V.; Leardi, R.; Farinini, E.; Fronza, G.; Menichini, P.; Monti, P.; Monteleone, L.; Valenti, G.E.; et al. Potential Role of miRNAs in the Acquisition of Chemoresistance in Neuroblastoma. *J. Pers. Med.* **2021**, *11*, 107. https://doi.org/10.3390/jpm11020107

Academic Editors: Sabata Martino and Chiara Villa
Received: 18 December 2020
Accepted: 4 February 2021
Published: 7 February 2021



## 1. Introduction

Neuroblastoma (NB) is an extracranial pediatric tumor originating from the aberrant development of neural crest-derived sympathoadrenal lineage [1], and is characterized by a high clinical and biological heterogeneity [2]. In fact, NB can be classified as a low-risk tumor, capable of spontaneously regressing, as well as a high-risk tumor, responsible for a high mortality rate and characterized by the presence of metastases.

The therapy used in high-risk patients is multimodal, and although the response to treatments is initially positive, subsequently, following the onset of chemoresistance, a large number of patients die as a consequence of relapse and metastasis formation [3]. NB metastasizes in vascularized tissue, and bone marrow (BM) is the preferential site of

recurrence, being considered as the "fertile soil" for tumor cells and, in particular, for the chemoresistant cells [4,5]. In fact, BM spread is considered a negative prognostic factor [6].

Among the prognostic markers of poor patient outcome, the amplification of the *MYCN* oncogene characterizes the most aggressive high-risk NB subtype [7,8]. More than ten years ago, it was proposed that another approach to classifying the risk group of NB patients could be to evaluate the expression levels of miRNAs [9]. Considering that *MYCN* modulates the expression of several miRNAs [10], the evaluation of these small non-coding RNA sequences has become an accurate predictor of NB outcome [11].

Furthermore, since miRNA expression is related to tumor grade, metastasis, and chemoresistance, they could represent a new class of potential therapeutic targets. In this context, we have recently demonstrated in an NB cell line-based model [12] that Etoposide resistance is associated with miRNA-15a/16-1 down-regulation, highlighting that miRNAs could have a role as both markers of chemoresistance and new possible therapeutic targets [13]. Therefore, in the present study, the expression of these miRNAs, amongst others, was analyzed in primary tumors, metastases, and bone marrow of therapy responder and non-responder NB patients in order to identify the specific miRNAs involved in NB progression and chemoresistance.

## 2. Materials and Methods

### 2.1. Cell Cultures

The *MYCN*-amplified human stage-IV NB cell line, HTLA-230, was obtained from Dr. L. Raffaghello (G. Gaslini Institute, Genoa, Italy), while the Etoposide-resistant cell line (ER-HTLA) was selected as previously reported [12,13]. Cells were periodically tested for mycoplasma contamination (Mycoplasma Reagent Set, Aurogene s.p.a, Pavia, Italy). Cells were cultured in RPMI 1640 (Euroclone SpA, Pavia, Italy) and supplemented with 10% fetal bovine serum (FBS; Euroclone SpA, Pavia, Italy), 2 mM of glutamine (Euroclone SpA, Pavia, Italy), 1% penicillin/streptomycin (Euroclone SpA, Pavia, Italy), 1% sodium pyruvate (Sigma-Aldrich, Saint Louis, MO, USA), and 1% amino acid solution (Sigma-Aldrich, Saint Louis, MO, USA).

### 2.2. Patient Samples

The patients included in the study were diagnosed with NB stage M between January 2002 and December 2015. Written consent for the use of samples and clinical data for research was obtained by their legal guardians. The study was approved by the Gaslini Institute Ethical Committee, and all analyses were performed according to the Helsinki declaration.

The samples used originated from two groups of patients. With regard to the first group, whole bone marrow (BM) samples were collected in PAXgene™ Blood RNA tubes originating from patients who, after diagnosis, were treated according to the high-risk European protocol. The drugs used in the induction therapy were Cisplatin, Etoposide, Vincristine, Cyclophosphamide, and either Carboplatin or Adriamycin. Patients were divided into two subgroups, responders and non-responders: responders being the patients that could proceed with high-dose chemotherapy and stem cell transplants, and non-responders being the patients who could not proceed and were referred to second-line therapy.

With regards to the second group, the samples were represented by tumor specimens containing more than 70% of neoplastic cells and immune-selected metastases from BM samples, as described [14,15] and containing 95% tumor cells. All patient samples were taken at diagnosis before starting with the treatment.

### 2.3. RNA Extraction

Total RNA was extracted from cultured cells using TRIZOL reagent (LifeTechnologies, Carlsbad, CA, USA) according to the manufacturer's instructions. Total RNA (1 µg) was reverse-transcribed into cDNA by a random hexamer primer and SuperScript™ II Reverse Transcriptase (LifeTechnologies, Carlsbad, CA, USA).

Total RNA and miRNA fractions were extracted from tumor cells and metastases using the miRNeasyMini kit (Qiagen, Hilden, Germany), according to the manufacturer's protocols. Total RNA and miRNA fractions were extracted from whole BM samples using the PAXgene extraction Kit (Qiagen, Hilden, Germany), according to manufacturer's protocol. The quality of the RNA fractions was evaluated in the BioAnalyzer 2100 system (Agilent Technologies, Santa Clara, CA, USA).

### 2.4. MiRNA Microarray Analysis

MiRNA expression profiling was carried out by the Agilent platform following the miRNA Microarray protocol v.3.1.1 (Agilent Technologies, Santa Clara, CA, USA). Briefly, 50 ng of total RNA, containing miRNAs and spike-in controls, underwent dephosphorylation and a labeling step with Cyanine 3-pCp. The Cy3-labeled RNA was then purified using the Micro Bio-Spin P-6 Gel Column (Bio-Rad Laboratories, Inc., Hercules, CA, USA), and hybridized on human miRNA microarray slides 8 × 60 K (Agilent Technologies; including 2549 miRNAs, miRBase 21.0) at 55 °C for 20 hours. After washing, the slides were scanned by a G2565CA scanner (Agilent Technologies, Santa Clara, CA, USA), and the images were extracted by Feature Extraction software v.10 (Agilent Technologies, Santa Clara, CA, USA). Tab-delimited text files were analyzed in R v.2.7.2 software environment http://www.r-project.org using the limma package v.2.14.16 of Bioconductor http://www.bioconductor.org. Only spots with a signal minus background flagged as positive and significant were used in the following analysis as detected spots. Probes with less than 50% of detected spots across all arrays and arrays with a number of detected spots smaller than 50% of all spots on the array were removed. Background corrected intensities of replicated spots on each array were averaged. Data were then log2-transformed and normalized for between-array comparison using quantile normalization [16]. MicroRNAs with $p$-values < 0.05 were selected for further analysis. Given the explorative nature of this study, no correction for multiple testing was applied to the screening procedure aimed at selecting multiple sets of microRNAs for subsequent hierarchical clustering analyses. The agglomerative hierarchical clusters, used to detect similarity relationships in microRNA log2-transformed expressions, were computed by the Euclidean distance between single vectors and the Ward method [17].

### 2.5. Real Time PCR Analysis

Total RNA (10 ng) was reverse transcribed using miR-specific stem-loop RT primers (TaqMan MicroRNA Assays; Applied Biosystems, Thermo-Fisher, Waltam, MA, USA) and components of the High Capacity cDNA Reverse Transcription kit (Life Technologies, Carlsbad, CA, USA), according to the manufacturer's protocols. Expression levels of individual miRNAs were detected by subsequent RQ-PCR using TaqMan MicroRNA assays (Life Technologies, Carlsbad, CA, USA) and a Rotor Gene 3000 PCR System Corbett (Qiagen, Hilden, Germany) with standard thermal cycling conditions, in accordance with manufacturer recommendations. PCR reactions were performed in triplicate in final volumes of 30 µl, including inter-assay controls (IAC) to account for variations between runs. RT-PCR (TaqMan MicroRNA Assays; Applied Biosystems, Thermo-Fisher) was used to quantify the expression of has-miR-16, has-miR-15a, has-miR-19b, has-miR-26b, has-miR-27b, has-miR-29c, has-miR-34c, has-miR-126, has-miR-218, has-miR-338, and has-miR-497, according to the manufacturer's instructions. To normalize the data for quantifying miRNAs, the universal small nuclear RNU38B (RNU38B Assay ID 001004; Applied Biosystems, Thermo-Fisher, Waltam, MA, USA) as an endogenous control was used [18].

The delta–delta Ct method was employed to calculate the fold change. In brief, each 15 µL of the reaction system contained 0.15 µL of 100 mM dNTPs with dTTP, 1 µL of MultiScribe Reverse Transcriptase (50 U/µL), 1.5 µL of RT buffer (×10), 0.1 µL of RNase inhibitor (20 U/µL), 6.25 µL of nuclease-free water, 5 µL of small RNA, and 3 µL of RT primer. Small RNAs were quantified by a Qubit 3 fluorimeter (Life Technologies, Carlsbad,

CA, USA). Thermal cycling conditions were 30 min at 16 °C, 30 min at 42 °C, and 5 min at 85 °C. Each 20 µL of the reaction system for real-time quantitative PCR contained 1 µL of real-time primer, 1.33 µL of product from the RT reaction, 10 µL of TaqMan Universal PCR Master Mix, and 7.67 µL of nuclease-free water. The reactions were performed in triplicate on a Rotor Gene 3000 PCR System Corbett for 10 min at 95 °C, followed by 40 cycles of 15 s at 95 °C and 1 min at 60 °C. Along with the Cq values calculated automatically by the SDS software (threshold value = 0.2, baseline setting: cycles 3–15), raw fluorescence data (Rn values) were exported for further analyses.

### 2.6. Comparative Genomic Hybridization (CGH) Analysis

Array CGH analyses were performed using the Human Genome array-CGH 8 × 60 K Microarray (Agilent Technologies, Palo Alto, CA), with an average probe spacing of around 55 Kb.

The arrays were performed using Agilent Reference DNAs, analyzed with the Agilent Microarray Scanner Feature Extraction Software version 11.5, and Agilent Genomic Workbench 7.0.4.0 software using the ADM-2 algorithm. Genomic positions of the rearrangements refer to the public UCSC database GRCh37.

### 2.7. PCA Analysis

Principal components analysis (PCA) is a data display method for multivariate data.

Given a data set in which each sample is described by $n$ variables, the PCA aims to find new directions and linear combinations of the original ones [19,20].

The first component (PC1) corresponds to the direction explaining the maximum variance, while PC2 is the direction, orthogonal to PC1, explaining the maximum variance not explained by PC1, and so on. The result of such a transformation is that a limited number of components is sufficient to explain the relevant part of the information.

The loadings are the coefficients of the linear combinations corresponding to the PCs. By plotting them in a loading plot, it is possible to understand the relationships among the variables in the multivariate space.

On the other side, the score plot (the scores being the coordinates of the samples in the new space defined by the PCs) allows the visualization of the location of samples in the space described by the PCs, making it possible to check similarities and differences among the samples.

The elaborations and the plots were carried out through the software CAT (Chemometric Agile Tool, www.gruppochemiometria.it) [21].

### 2.8. Statistical Analysis

Results were expressed as mean ± SEM from at least three independent experiments. The statistical significance of the parametric differences among the sets of experimental data was evaluated by one-way ANOVA and Dunnett's test for multiple comparisons. Statistical analysis of the mitotic index and reporter assays data was performed using the Fisher's exact test.

## 3. Results and Discussion

### 3.1. miRNA Expression Profiling of HTLA-230 and ER-HTLA Cells.

In order to identify the miRNAs involved in chemoresistance, miRNA microarray analyses were performed on HTLA-230 and ER-HTLA cells.

As shown in Figure 1, miRNAs were differently expressed when comparing these two cell populations. The scatter plot analysis showed that a total of 152 miRNAs changed their expression more than 1.5 fold, 41 being up-regulated and 111 down-regulated (Figure 1).

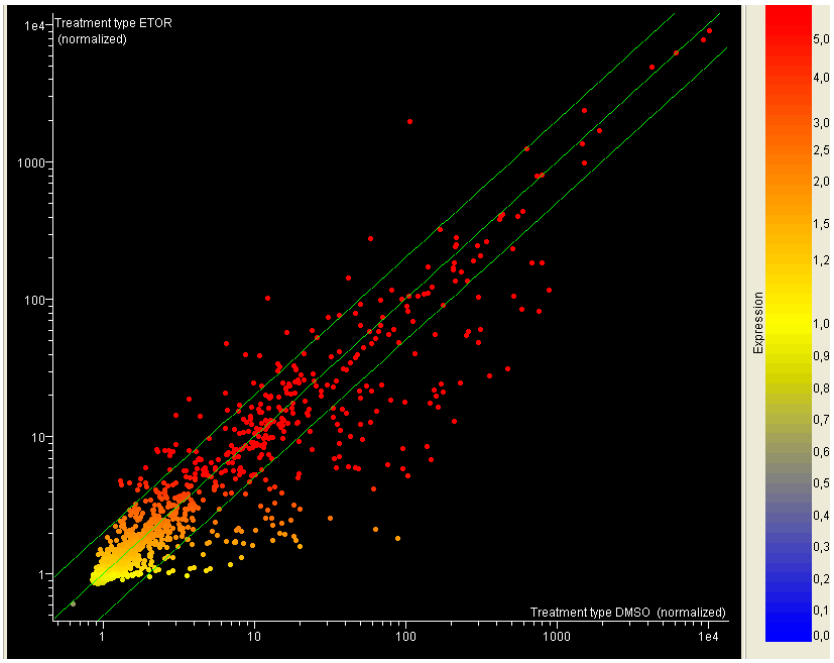


**Figure 1.** Scatter plot analysis reporting the variation of miRNA expression between HTLA-230 (horizontal axis) and ER-HTLA cells (vertical axis). Each dot represents one miRNA colored according to its level of expression. Green diagonal lines indicate the 1.5-fold variation interval.

Volcano plot analyses, considering threshold values of five-fold for fold variation and $p < 0.01$ for statistical significance, showed that a total of 35 miRNAs significantly changed their expression, three being up-regulated and 32 down-regulated. The list of these 35 miRNAs is available in the Supplementary Material (Table S1).

Given the mechanism of action of miRNAs in regulating gene expression, we focused our attention on the down-regulated ones, and, in order to restrict the number of miRNAs to be studied, from the literature we searched for miRNAs that had been specifically involved in NB biology and/or chemoresistance. Using this criterion, 11 miRNAs were selected (Table 1), and their expression was tested by RT-qPCR analysis.

**Table 1.** miRNAs differently expressed in HTLA-230 and ER-HTLA cell lines that are involved in NB biology and in general cancer chemoresistance.

| miRNA | HTLA-230/ ER-HTLA Ratio | Expression in Neuroblastoma | Expression in Other Chemoresistant Cancers |
|---|---|---|---|
| miR-15a | 11.38 | Down-regulated in *MYCN*-amplified chemoresistant NB [13,22–24] | Down-regulated in Burkitt Lymphoma [25], pancreatic ductal adenocarcinoma [26], colorectal [27], and ovarian cancer [28] |
| miR-16 | 7.89 | Down-regulated in *MYCN*-amplified NB [22,29] and in chemoresistant NB [13] | Down-regulated in cervical [30], breast [31,32] gastric [32,33], and lung [34] cancer, osteosarcoma [35], and mesothelioma [36] |
| miR-19b | 7.75 | Up-regulated in chemoresistant NB [37] | Down-regulated in breast [38] and colon [39] cancer and leukemia [40] |
| miR-26b | 47.87 | Not evaluated | Down-regulated in chemoresistant colorectal [41], gastric [42], laryngeal [43], and hepatocellular carcinoma [44,45] cancer and in glioma [46] |

**Table 1.** *Cont.*

| miRNA | HTLA-230/ ER-HTLA Ratio | Expression in Neuroblastoma | Expression in Other Chemoresistant Cancers |
|---|---|---|---|
| miR-27b | 8.29 | Down-regulated in NB [47] | Down-regulated in lung [48], breast [49], and gastric cancer [50] |
| miR-29c | 9.27 | Not evaluated | Down-regulated in ovarian [51], endometrial [52], gastric [53], and small cell lung [54] cancer, glioma [55,56], and leukemia [57,58] |
| miR-34c | 7.49 | Not evaluated | Down-regulated in colon [59], gastric [60,61], and ovarian [62,63] cancer, and osteosarcoma [64] |
| miR-126a | 9.66 | Not evaluated | Down-regulated in colorectal [65] and breast cancer [66] and in renal cell carcinoma [67] |
| miR-218 | 12.30 | Up-regulated in *MYCN*-amplified and in metastatic NB [68–70] | Down-regulated in glioma cells [71], colorectal [72], gallbladder [73], bladder [74], and lung cancer [75,76] |
| miR-338 | 15.99 | Down-regulated in resistant NB [77,78] | Down-regulated in esophageal squamous carcinoma cells [79] |
| miR-497 | 6.92 | Down-regulated in chemoresistant NB [24], in *MYCN*-amplified NB [80] | Down-regulated in lung [81], colorectal [82], ovarian [83], and pancreatic [84] cancer, and lymphoma [85] |

As shown in Figure 2, only six miRNAs (i.e., miR-15a, -16-1, -19b, -27b, -126, and -218) among the selected miRNAs were confirmed to be down-regulated in ER-HTLA cells in respect to HTLA-230 parental ones. In detail, miR-27b and miR-16-1 expression levels were found to be reduced by 33.1 and 23.5 fold, respectively, and miR-218 expression was diminished by 9.09 fold, while miR-15a, miR-126, and miR-19b were down-regulated (slightly, but significantly) by 2.8, 2.7, and 1.73 fold, respectively.

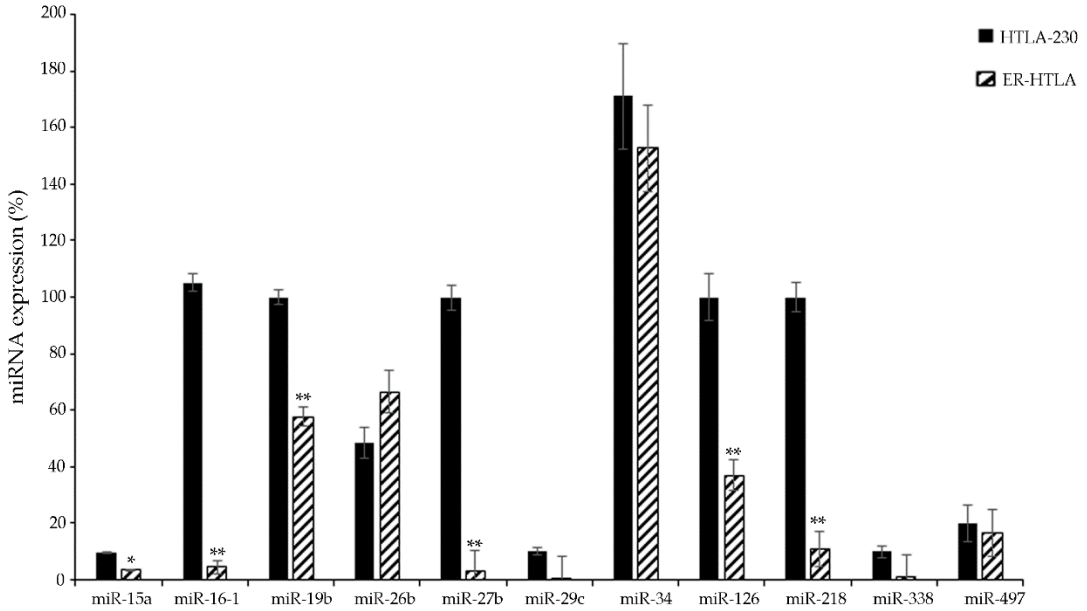


**Figure 2.** Evaluation of the expression level of the 11 selected miRNAs (Table 1) in HTLA-230 and ER-HTLA cell lines by RT-qPCR analysis. Data is reported as % variation vs. the universal small nuclear RNU38B. * $p < 0.05$ vs. HTLA-230 ** $p < 0.01$ vs. HTLA-230.

For the first time, to our knowledge, this data confers a possible role in NB chemoresistance to miR-27 and miR-218. In fact, despite their expression being found to be down-

regulated in several chemoresistant cancers (see Table 1) [48–50,71–75], their involvement in chemoresistance of NB has never been reported in the literature. Notably, although miRNA-218 was found to be up-regulated in *MYCN*-amplified and metastatic NB [68–70], this data is not in contradiction with the down-regulation of miRNA-218 that we have observed after chronic Etoposide exposure of *MYCN*-amplified NB cells (ER-HTLA).

In addition, these results confirm the down-regulation of miR-15 and miR-16 in ER-HTLA cells, as found in our previous study [13]. Moreover, for the first time, miR-19b expression was found to be reduced in chemoresistant NB in conformity with other malignancies (Table 1) [38–40]. In fact, only one study has reported an up-regulation of miR-19b in chemoresistant NB cells [37]. This discrepancy could be due to the fact that, in this same study, NB cells were exposed to the drug for only 24 hours while, in our present study, the ER-HTLA cells were selected by chronically treating parental cells (HTLA-230) with Etoposide for six months (i.e., a condition that better mimics in vivo treatment).

### *3.2. Comparative Genomic Hybridization (CGH) on HTLA-230 and ER-HTLA Cells*

Since both genetic and epigenetic mechanisms have been demonstrated to influence NB biology [86], in order to better characterize the chemoresistant phenotype, CGH analysis was performed. DNAs from HTLA-230 and ER-HTLA cells were hybridized to obtain a comparison of gains and losses that could be connected to the acquisition of chemoresistance. As reported in Table 2, an intriguing finding was the presence of several alterations in chromosome 13, where miR-15a, miR-16-1, and miR-19b were mapped, and, in chromosome 17, where miR-338 was localized.

**Table 2.** CGH analysis on HTLA-ER cells in comparison to HTLA-230 cells.

| CHR | START | STOP | CYTO | SIZE KB | VALUE | Control (HTLA-230) |
|---|---|---|---|---|---|---|
| **1** | 152,079,488 | 155,154,990 | q21.3–q22 | 3.075 | 1.5 | Absent |
| **3** | 73,792,065 | 75,028,724 | p13–p12.3 | 1.236 | −0.7 | Absent |
| **5** | 20,160,410 | 44,924,503 | p14.3–p12 | 24.764 | −0.7 | Absent |
| **8** | 112,697,432 | 146,280,020 | q23.3–q24.3 | 33.582 | −1/−0.4 | Duplicated |
| **9** | 204,193 | 38,815,475 | p24.3–p13.1 | 38.611 | −0.7/−3 | Absent |
| **10** | 43,020,732 | 60,914,512 | q11.21–q21.1 | 17.893 | −0.7/−1.2 | Duplicated |
| **12** | 38,805,636 | 48,103,580 | q12–q13.11 | 9.297 | 0.7/0.4/1.4 | Absent |
| **13** | 20,412,619 | 39,841,779 | q12.11–q13.3 | 19.429 | 0.3/0.6 | Absent |
| **13** | 39,900,189 | 86,110,407 | q13.3–q31.1 | 46.210 | −0.5 | Absent |
| **13** | 86,151,801 | 111,106,213 | q31.1–q34 | 24.954 | 0.5 | Absent |
| **13** | 111,181,035 | 113,538,619 | q34 | 2.357 | −0.8 | Absent |
| **13** | 113,610,612 | 115,092,648 | q34 | 1.482 | 0.4 | Absent |
| **17** | 44,684 | 625,475 | p13.3 | 580 | −0.7 | Absent |
| **17** | 25,654,874 | 40,109,636 | q11.1–q21.2 | 14.454 | −0.7/−1.2 | Duplicated |
| **19** | 32,783,771 | 36,293,337 | q13.11–q13.12 | 3.509 | −0.6 | Duplicated |
| **20** | 60,747 | 19,483,849 | p13–p11.23 | 19.423 | 0.5 | Deleted or mosaic |
| **21** | 15,538,980 | 32,776,404 | q11.2–q22.11 | 17.237 | −0.6 | Absent |

Moreover, our data, identifying some chromosomal regions that are more frequently altered in ER-HTLA cells, is in line with the results obtained in a previous paper reporting a gain of 13q14.1-32 and a loss of 17q in other NB chemoresistant cell lines [87]. Since these chromosome traits (e.g., chromosome 13) contain the locus in which miRNAs, involved in the acquisition of Etoposide resistance, are mapped, it is possible to hypothesize that the evaluation of these miRNAs in patient samples might be used as prognostic markers that are able to early identify chemoresistant signatures.

### 3.3. miRNA Expression Profiling of Therapy-Sensitive (Responder) and Therapy-Resistant (Non-Responder) NB Patients

In order to evaluate in vivo the expression of miRNAs and their potential role in NB chemoresistance, ten whole BM samples, taken at diagnosis from NB patients either sensitive (responder) or resistant (non-responder) to induction therapy, were randomly selected from our biobank, and six miRNAs from Table 1 (i.e., miR-15a, -16-1, 19b, -27b, -126, and -218) were analyzed. NB patient characteristics are reported in Table 3.

**Table 3.** NB characteristics and patient clinical outcomes.

| N | MYCN Status | Age (Months) | EFS (Months) | OS (Months) | INRG Stage | Induction Response | Relapse | Follow-Up |
|---|---|---|---|---|---|---|---|---|
| 2 | Amplified | 55 | 71.25 | 71.25 | M | Yes | No | Alive |
| 3 | Not evaluated | 41 | 81.06 | 81.06 | M | Yes | No | Alive |
| 4 | Single copy | 12 | 60.53 | 60.53 | M | Yes | No | Alive |
| 6 | Amplified | 62 | 50.83 | 50.83 | M | Yes | No | Alive |
| 9 | Amplified | 21 | 55.38 | 55.38 | M | Yes | No | Alive |
| 1 | Amplified | 17 | 6.86 | 7.10 | M | No | Yes | Dead |
| 5 | Single copy | 47 | 22.94 | 26.17 | M | No | Yes | Dead |
| 7 | Amplified | 20 | 9.54 | 19.27 | M | No | Yes | Dead |
| 8 | Amplified | 21 | 5.54 | 7.00 | M | No | Yes | Dead |
| 10 | Amplified | 16 | 4.69 | 8.98 | M | No | Yes | Dead |

EFS, event-free survival; OS, overall survival; INRG, International Neuroblastoma Risk Group.

By comparing the expression of miRNAs in therapy-sensitive and therapy-resistant NB patients, only miR-16 was significantly down-regulated in the bone marrow of non-responder patients (Figure 3), while the other miRNAs analyzed were not significantly modified, even though a slight trend of reduction in non-responder patients was observed.

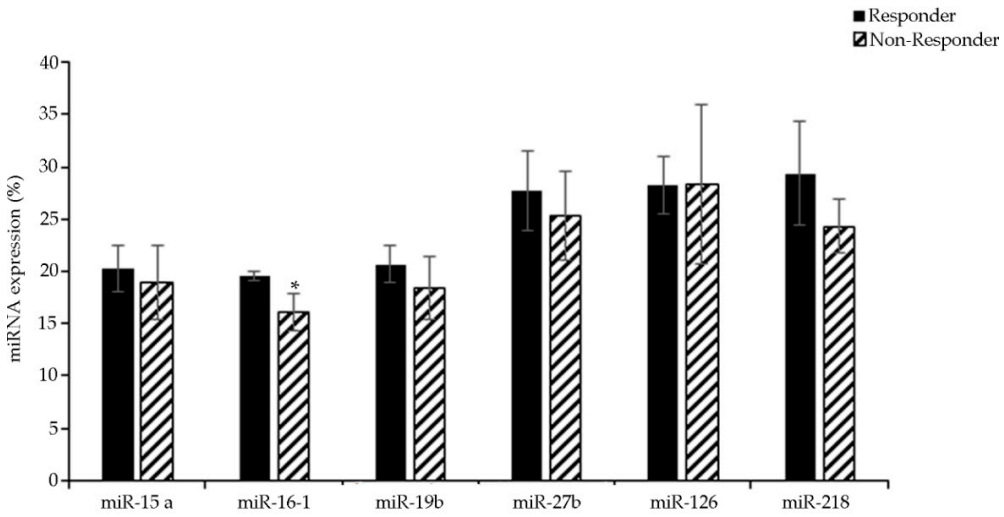


**Figure 3.** Evaluation of the expression levels of selected miRNAs in the bone marrow of patients sensitive (responder) or resistant (non-responder) to therapy by RT-qPCR analysis. Data is reported as % variation vs. the universal small nuclear RNU38B. * $p < 0.05$ vs. responder.

These findings, while confirming a potential role of miR-16 in delivering intrinsic chemoresistance of NB, do not confirm the other results obtained from ER-HTLA cells. However, this is not unusual when comparing in vitro with in vivo data, most likely due to the variability found in individual patients. Nevertheless, it should be noted that

the content of NB cells in the BM samples ranged from 5% to 35%, making the normal hematopoietic cells prevalent, and thus potentially masking miRNA down-regulation occurring in neoplastic cells.

### 3.4. miRNA Expression Profiling of NB Primary Tumors and Metastases

Therefore, in order to better understand the role that these miRNAs could possibly have in NB biology, their expression was tested in ten primary tumors and ten immune-magnetically-enriched NB metastases from stage M NB patients, randomly selected from our biobank. The NB patients' features of this new set of samples are reported in Table 4. Since it has been recently reported [13] and herein confirmed that ER-HTLA cells have a monoallelic deletion of the 13q14.3 locus, which maps for miR-15/16, particular attention was given to those miRNAs whose locus was found mutated. The analysis was also extended to miR-338 and miR-218, even though the corresponding locus had not been altered, because their expression has been demonstrated to be strictly related to NB chemoresistance [77,78] and to Etoposide refractoriness [76].

**Table 4.** Features of NB primary tumors and metastases and patients' clinical outcomes.

| | N | MYCN Status | Age (Years) | EFS (Months) | OS (Months) |
|---|---|---|---|---|---|
| Tumors | 1 | Amplified | 1.99 | 46.2 | 84.8 |
| | 2 | Not amplified | 3.18 | 5.3 | 9.3 |
| | 3 | Not amplified | 1.27 | 187.2 | 187.2 |
| | 4 | Amplified | 1.13 | 4.3 | 7.4 |
| | 5 | Amplified | 3.88 | 70.0 | 114.5 |
| | 6 | Amplified | 6.30 | 36.2 | 47.7 |
| | 7 | Amplified | 2.07 | 3.2 | 10.3 |
| | 8 | Amplified | 4.76 | 114,9 | 114,9 |
| | 9 | Amplified | 4.57 | 21.7 | 22.4 |
| | 10 | Amplified | 1.44 | 26.8 | 33.0 |
| Metastases | 11 | Not amplified | 1.68 | 58.88 | 58.88 |
| | 12 | Not amplified | 3 | 24.52 | 35.98 |
| | 13 | Amplified | 6.8 | 8.68 | 42.41 |
| | 14 | Amplified | 0.9 | 11.06 | 11.06 |
| | 15 | Not amplified | 2.55 | 70.73 | 70.73 |
| | 16 | Not amplified | 3.34 | 13,3 | 21.22 |
| | 17 | Amplified | 8.2 | 8.61 | 8.61 |
| | 18 | Amplified | 1.67 | 9.6 | 14.98 |
| | 19 | Amplified | 6.89 | 29.04 | 29.04 |
| | 20 | Amplified | 1.7 | 13.3 | 23 |

EFS, event-free survival; OS, overall survival.

As reported in Figure 4, miRNA-19b, -218, and -338 were down-regulated in *MYCN*-amplified metastases by about 30% as compared to *MYCN*-amplified tumors, while no significant changes were observed in the expression of the other miRNAs. It is interesting to note that the *MYCN* status did not influence the expression of these latter miRNAs, neither in tumors nor in metastases (Figure 4).

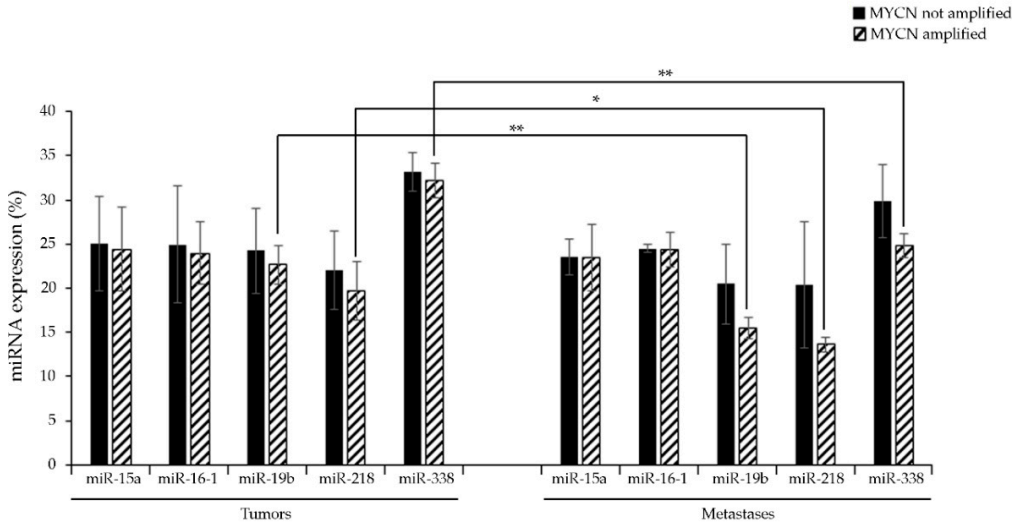


**Figure 4.** RT-qPCR analysis of the selected miRNA expression levels in tumors and metastases samples of NB patients. Data is reported as % variation vs. the universal small nuclear RNU38B. * $p < 0.05$ vs. *MYCN*-amplified tumors; ** $p < 0.01$ vs. *MYCN*-amplified tumors.

miR-338 down-regulation in NB metastases has been previously reported by Chen et al., who demonstrated that this miRNA could exert an inhibitory role on the migration, proliferation, and invasion of NB cells through the modulation of the PTEN/Akt pathway [77]. However, while miR-19b expression has been found to be reduced in metastatic clear renal cell carcinoma [88] and miR-218 expression down-regulated in metastatic prostate [89], breast [90], gastric [91], cervical [92], and lung [93] cancer, to our knowledge, this is the first time that a down-regulation of miR-19b has been detected in metastatic NB in vivo. In addition, miRNA-218 has also been found to be down-regulated in NB metastases. This result obtained from analyses of patients' tissues is in contrast with previous studies reporting an up-regulation of this miRNA [70] in patients' serum, but this discrepancy could be due to the different nature of the analyzed samples. In fact, it is conceivable that the increased levels of miRNA-218 in the serum might be due to a response of peritumoral tissue, and not originating from the tumor.

### *3.5. Principal Component Analysis (PCA) of the Results Obtained in Patients' Samples*

In order to better extract the information from the dataset about NB biology and chemoresistance, principal component analysis (PCA) was carried out by collecting miRNA expression profiles analyzed in bone marrows infiltrates, tumors, and metastases. The first PCA has been performed on responder (four) and non-responder (four) patients' samples. The loading plot showed that all of the variables had similar positive loadings on PC1, meaning that the score on PC1 can be considered as a global quantitative index. On the other hand, PC2 mainly explains the contrast between miR-15, miR-218, and -16 variables (Figure 5, left panel). By analyzing the score plot, although only a few subjects were available, it was possible to observe that all of the responder patients' samples (red) were well-separated from the non-responders (black) and located in a specific region in the PC space: compared to the non-responders, all of the responders were mainly characterized by higher values of the variables miR-218 and miR-16 (Figure 5, right panel).

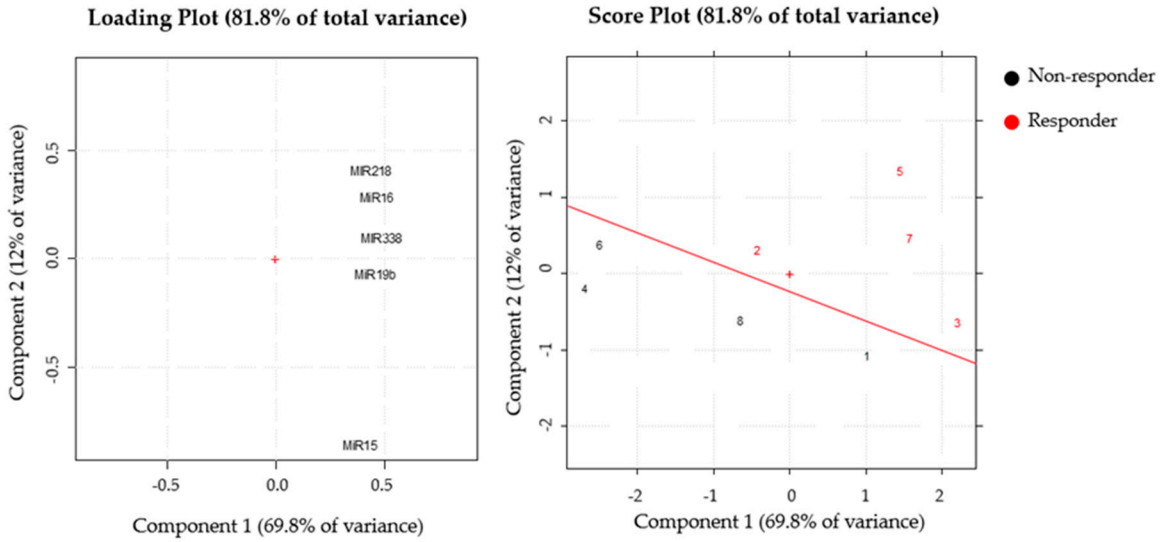


**Figure 5.** PCA performed on responder and non-responder patients' samples. The loading (left panel) and the score plot (right panel) were reported. In the score plot, the samples were indicated by the number reported in Table 3. + represents the point with coordinates 0 and 0 for x and y axes, respectively. This points is the reference to define the multivariate space.

Furthermore, a second PCA was carried out on tumor and metastasized patients' samples. The loading plot showed correlations between the variables miR-19b, -218, and -338, all characterized by negative loadings on PC1 (group 1), and between miR-15 and -16, which had positive loadings on PC2 (group 2). The two groups of correlated variables were uncorrelated, since their directions from the origin were orthogonal (Figure 6, left panel). The score plot showed that the metastasized patients' samples were characterized by intermediate values of the variables miR-15 and -16. On the other hand, the majority of the non-metastasized patients' samples had extreme values of both variables miR-15 and -16 (Figure 6, right panel).

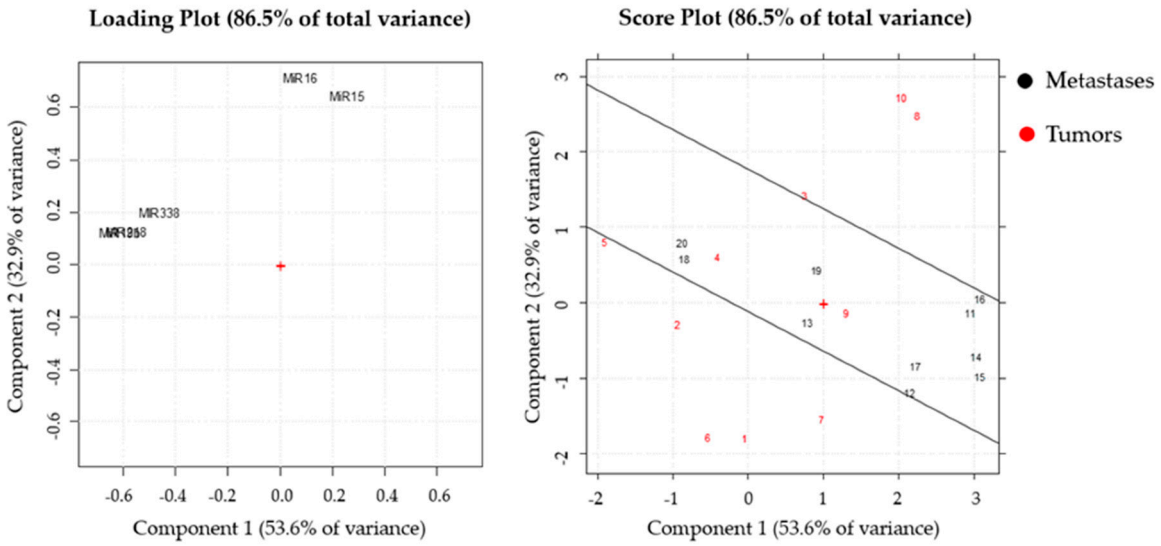


**Figure 6.** PCA performed on tumors and metastases samples. The loading (left panel) and the score plot (right panel) were reported. In the score plot, the samples were indicated by the number reported in Table 4. + represents the point with coordinates 0 and 0 for x and y axes, respectively. This points is the reference to define the multivariate space.

## 4. Conclusions

The presence of chemoresistant cells in the primary tumor and within bone marrow is the most powerful negative prognostic factor for patients with NB. The acquisition of chemoresistance and the ability to metastasize are the results of genetic and epigenetic mechanisms and, among them, miRNAs can play a crucial role [94]. In fact, their expression is frequently de-regulated in several chemoresistant malignancies and, as supported by the results herein, in NB. Indeed, the evaluation of miRNA expression could have a double value. In fact, on the one hand, the modulation of a specific miRNA or of a cluster of miRNAs could be used as a prognostic and predictive factor advantageous for monitoring the acquisition of chemoresistance. On the other hand, miRNAs might also have therapeutic potential, since many current studies are focused on discovering the best mechanism that is able to restore the expression of miRNAs in oncologic patients [95]. In the present study, our findings demonstrate, for the first time, that the down-regulation of miR-16-1 is strictly related to the acquisition of NB chemoresistance. In fact, among the six miRNAs whose expression is found down-regulated in our in vitro model of Etoposide resistance, only miR-16-1 is significantly down-regulated in non-responder NB patients treated with the induction therapy comprised of Etoposide (Figure 7). This data suggests that the restoration of miR-16 could be a valid strategy to counteract chemoresistance (Figure 7).

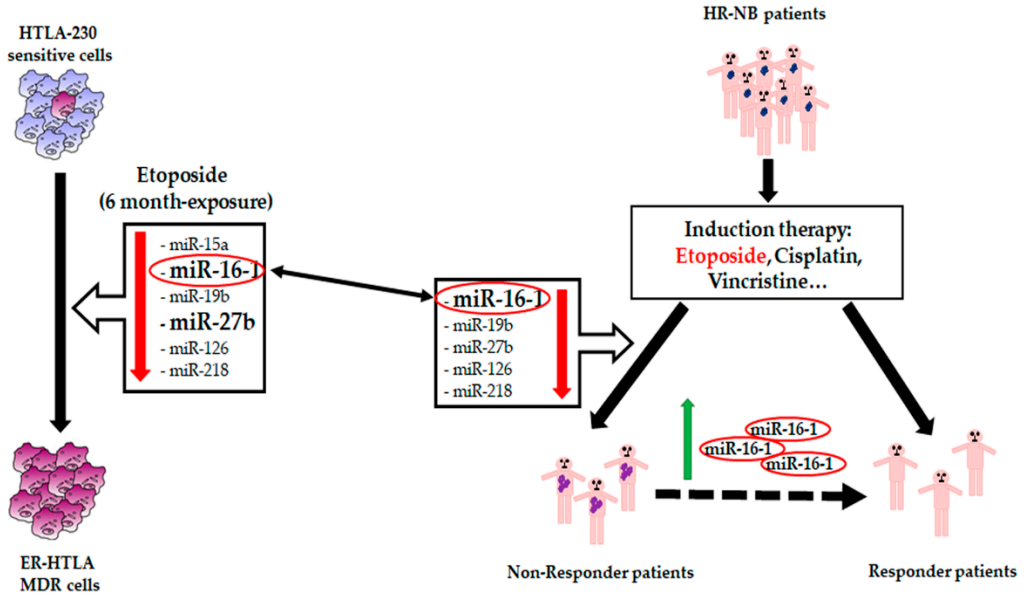


**Figure 7.** Role of miR-16-1 in NB chemoresistance. The acquisition of chemoresistance in multidrug resistant (MDR) cells and in high-risk (HR) patients is characterized by miR-16-1 down-regulation, suggesting a potential role of miR-16-1 as a chemosensitizer.

In addition, miR-19b, miR-338, and partially miR-218, whose down-regulation correlates with the metastatic process, could have prognostic value as biomarkers of NB progression.

**Supplementary Materials:** The following are available online at https://www.mdpi.com/2075-4426/11/2/107/s1, Table S1: miRNAs differently expressed in HTLA-230 and ER-HTLA cells.

**Author Contributions:** Conceptualization, B.M., A.P., M.V.C., A.I., and C.D.; methodology, B.M., A.P., and M.V.C.; validation, G.F., P.M., P.M., and A.S.; formal analysis, B.M., A.P., R.L., and E.F.; investigation, B.M., A.P., M.V.C., L.M., G.E.V., P.P., and F.M.; resources, B.M., A.P., A.I., and C.D.; data curation, B.M., A.P., A.I., and C.D.; writing—original draft preparation, B.M., A.P., M.V.C., G.F., P.M. (Paola Menichini), and P.M. (Paola Monti); writing—review and editing, B.M., A.I., and C.D.; visualization, B.M., A.P., M.V.C., and F.M.; supervision, B.M. and C.D.; project administration, B.M., A.I., and C.D.; funding acquisition, B.M. and C.D. All authors have read and agreed to the published version of the manuscript.

**Funding:** This research was supported by the University of Genoa and by the Italian Association for Cancer research (AIRC) IG-2017 Id.20699.

**Institutional Review Board Statement:** The study was approved by the Gaslini Institute Ethical Committee and all analyses were performed according to the Declaration of Helsinki.

**Informed Consent Statement:** Informed consent was obtained from all subjects involved in the study.

**Data Availability Statement:** Data are available upon request from the corresponding author. Data are not publicly available due to patients'privacy.

**Acknowledgments:** We would like to thank Giuseppe Catalano (DIMES-University of Genoa) for his technical assistance and Suzanne Patten for her language editing.

**Conflicts of Interest:** The authors declare no conflict of interest.

## References

1. Maris, J.M. Recent advances in neuroblastoma. *N. Engl. J. Med.* **2010**, *362*, 2202–2211. [CrossRef] [PubMed]
2. Brodeur, G.M. Neuroblastoma: Biological insights into a clinical enigma. *Nat. Rev. Cancer* **2003**, *3*, 203–216. [CrossRef] [PubMed]
3. Pinto, N.R.; Applebaum, M.A.; Volchenboum, S.L.; Matthay, K.K.; London, W.B.; Ambros, P.F.; Nakagawara, A.; Berthold, F.; Schleiermacher, G.; Park, J.R.; et al. Advances in Risk Classification and Treatment Strategies for Neuroblastoma. *J. Clin. Oncol.* **2015**, *33*, 3008–3017. [CrossRef]
4. Hochheuser, C.; van Zogchel, L.M.J.; Kleijer, M.; Kuijk, C.; Tol, S.; van der Schoot, C.E.; Voermans, C.; Tytgat, G.A.M.; Timmerman, I. The Metastatic Bone Marrow Niche in Neuroblastoma: Altered Phenotype and Function of Mesenchymal Stromal Cells. *Cancers* **2020**, *12*, 3231. [CrossRef]
5. Seeger, R.C.; Reynolds, C.P.; Gallego, R.; Stram, D.O.; Gerbing, R.B.; Matthay, K.K. Quantitative tumor cell content of bone marrow and blood as a predictor of outcome in stage IV neuroblastoma: A Children's Cancer Group Study. *J. Clin. Oncol.* **2000**, *18*, 4067–4076. [CrossRef] [PubMed]
6. Cai, J.Y.; Pan, C.; Tang, Y.J.; Chen, J.; Ye, Q.D.; Zhou, M.; Xue, H.; Tang, J.Y. Minimal residual disease is a prognostic marker for neuroblastoma with bone marrow infiltration. *Am. J. Clin. Oncol.* **2012**, *35*, 275–278. [CrossRef]
7. Stallings, R.L. Are chromosomal imbalances important in cancer? *Trends Genet.* **2007**, *23*, 278–283. [CrossRef]
8. Brodeur, G.M.; Seeger, R.C.; Schwab, M.; Varmus, H.E.; Bishop, J.M. Amplification of N-myc in untreated human neuroblastomas correlates with advanced disease stage. *Science* **1984**, *224*, 1121–1124. [CrossRef]
9. Lin, R.J.; Lin, Y.C.; Chen, J.; Kuo, H.H.; Chen, Y.Y.; Diccianni, M.B.; London, W.B.; Chang, C.H.; Yu, A.L. microRNA signature and expression of Dicer and Drosha can predict prognosis and delineate risk groups in neuroblastoma. *Cancer Res.* **2010**, *70*, 7841–7850. [CrossRef] [PubMed]
10. Schulte, J.H.; Schowe, B.; Mestdagh, P.; Kaderali, L.; Kalaghatgi, P.; Schlierf, S.; Vermeulen, J.; Brockmeyer, B.; Pajtler, K.; Thor, T.; et al. Accurate prediction of neuroblastoma outcome based on miRNA expression profiles. *Int. J. Cancer* **2010**, *127*, 2374–2385. [CrossRef]
11. Mohammadi, M.; Goodarzi, M.; Jaafari, M.R.; Mirzaei, H.R.; Mirzaei, H. Circulating microRNA: A new candidate for diagnostic biomarker in neuroblastoma. *Cancer Gene Ther.* **2016**, *23*, 371–372. [CrossRef]
12. Colla, R.; Izzotti, A.; De Ciucis, C.; Fenoglio, D.; Ravera, S.; Speciale, A.; Ricciarelli, R.; Furfaro, A.L.; Pulliero, A.; Passalacqua, M.; et al. Glutathione-mediated antioxidant response and aerobic metabolism: Two crucial factors involved in determining the multi-drug resistance of high-risk neuroblastoma. *Oncotarget* **2016**, *7*, 70715–70737. [CrossRef] [PubMed]
13. Marengo, B.; Monti, P.; Miele, M.; Menichini, P.; Ottaggio, L.; Foggetti, G.; Pulliero, A.; Izzotti, A.; Speciale, A.; Garbarino, O.; et al. Etoposide-resistance in a neuroblastoma model cell line is associated with 13q14.3 mono-allelic deletion and miRNA-15a/16-1 down-regulation. *Sci. Rep.* **2018**, *8*, 13762. [CrossRef] [PubMed]
14. Scaruffi, P.; Morandi, F.; Gallo, F.; Stigliani, S.; Parodi, S.; Moretti, S.; Bonassi, S.; Fardin, P.; Garaventa, A.; Zanazzo, G.; et al. Bone marrow of neuroblastoma patients shows downregulation of CXCL12 expression and presence of IFN signature. *Pediatr. Blood Cancer* **2012**, *59*, 44–51. [CrossRef]
15. Morandi, F.; Scaruffi, P.; Gallo, F.; Stigliani, S.; Moretti, S.; Bonassi, S.; Gambini, C.; Mazzocco, K.; Fardin, P.; Haupt, R.; et al. Bone marrow-infiltrating human neuroblastoma cells express high levels of calprotectin and HLA-G proteins. *PLoS ONE* **2012**, *7*, e29922. [CrossRef] [PubMed]
16. Stracquadanio, M.; Dinelli, E.; Trombini, C. Role of volcanic dust in the atmospheric transport and deposition of polycyclic aromatic hydrocarbons and mercury. *J. Environ. Monit.* **2003**, *5*, 984–988. [CrossRef]
17. Alexandrov, K.; Rojas, M.; Geneste, O.; Castegnaro, M.; Camus, A.M.; Petruzzelli, S.; Giuntini, C.; Bartsch, H. An improved fluorometric assay for dosimetry of benzo(a)pyrene diol-epoxide-DNA adducts in smokers' lung: Comparisons with total bulky adducts and aryl hydrocarbon hydroxylase activity. *Cancer Res.* **1992**, *52*, 6248–6253.

18. Torres, A.; Torres, K.; Wdowiak, P.; Paszkowski, T.; Maciejewski, R. Selection and validation of endogenous controls for microRNA expression studies in endometrioid endometrial cancer tissues. *Gynecol. Oncol.* **2013**, *130*, 588–594. [CrossRef]
19. Davies, T.; Fearn, T. *Back to Basics: The Principles of Principal Component Analysis*; Spectroscopy Europe: Charlston, Chichester, UK, 2004; p. 20.
20. Leardi, R. Chemometric methods in food authentication. In *Modern Techniques for Food Authentication*, 2nd ed.; Elsevier: Amsterdam, The Netherlands, 2018; pp. 687–729.
21. Leardi, R.; Melzi, C.; Polotti, G. CAT (Chemometric Agile Software). Available online: http://gruppochemiometria.it/index.php/software (accessed on 18 December 2020).
22. Chava, S.; Reynolds, C.P.; Pathania, A.S.; Gorantla, S.; Poluektova, L.Y.; Coulter, D.W.; Gupta, S.C.; Pandey, M.K.; Challagundla, K.B. miR-15a-5p, miR-15b-5p, and miR-16-5p inhibit tumor progression by directly targeting MYCN in neuroblastoma. *Mol. Oncol.* **2020**, *14*, 180–196. [CrossRef]
23. Pouliot, L.M.; Chen, Y.C.; Bai, J.; Guha, R.; Martin, S.E.; Gottesman, M.M.; Hall, M.D. Cisplatin sensitivity mediated by WEE1 and CHK1 is mediated by miR-155 and the miR-15 family. *Cancer Res.* **2012**, *72*, 5945–5955. [CrossRef] [PubMed]
24. Soriano, A.; París-Coderch, L.; Jubierre, L.; Martínez, A.; Zhou, X.; Piskareva, O.; Bray, I.; Vidal, I.; Almazán-Moga, A.; Molist, C.; et al. MicroRNA-497 impairs the growth of chemoresistant neuroblastoma cells by targeting cell cycle, survival and vascular permeability genes. *Oncotarget* **2016**, *7*, 9271–9287. [CrossRef] [PubMed]
25. Guo, C.; Gong, M.; Li, Z. Knockdown of lncRNA MCM3AP-AS1 Attenuates Chemoresistance of Burkitt Lymphoma to Doxorubicin Treatment via Targeting the miR-15a/EIF4E Axis. *Cancer Manag. Res.* **2020**, *12*, 5845–5855. [CrossRef] [PubMed]
26. Guo, S.; Fesler, A.; Huang, W.; Wang, Y.; Yang, J.; Wang, X.; Zheng, Y.; Hwang, G.R.; Wang, H.; Ju, J. Functional Significance and Therapeutic Potential of miR-15a Mimic in Pancreatic Ductal Adenocarcinoma. *Mol. Ther. Nucleic Acids* **2020**, *19*, 228–239. [CrossRef] [PubMed]
27. Fesler, A.; Liu, H.; Ju, J. Modified miR-15a has therapeutic potential for improving treatment of advanced stage colorectal cancer through inhibition of BCL2, BMI1, YAP1 and DCLK1. *Oncotarget* **2017**, *9*, 2367–2383. [CrossRef]
28. Dwivedi, S.K.; Mustafi, S.B.; Mangala, L.S.; Jiang, D.; Pradeep, S.; Rodriguez-Aguayo, C.; Ling, H.; Ivan, C.; Mukherjee, P.; Calin, G.A.; et al. Therapeutic evaluation of microRNA-15a and microRNA-16 in ovarian cancer. *Oncotarget* **2016**, *7*, 15093–15104. [CrossRef]
29. Zhang, X.; Zhang, J.; Liu, Q.; Zhao, Y.; Zhang, W.; Yang, H. Circ-CUX1 Accelerates the Progression of Neuroblastoma via miR-16-5p/DMRT2 Axis. *Neurochem. Res.* **2020**, *45*, 2840–2855. [CrossRef]
30. Zhao, Z.; Ji, M.; Wang, Q.; He, N.; Li, Y. miR-16-5p/PDK4-Mediated Metabolic Reprogramming Is Involved in Chemoresistance of Cervical Cancer. *Mol. Ther. Oncolytics* **2020**, *17*, 509–517. [CrossRef]
31. Patel, N.; Garikapati, K.R.; Pandita, R.K.; Singh, D.K.; Pandita, T.K.; Bhadra, U.; Bhadra, M.P. miR-15a/miR-16 down-regulates BMI1, impacting Ub-H2A mediated DNA repair and breast cancer cell sensitivity to doxorubicin. *Sci. Rep.* **2017**, *7*, 4263. [CrossRef] [PubMed]
32. Venturutti, L.; Russo, R.I.C.; Rivas, M.A.; Mercogliano, M.F.; Izzo, F.; Oakley, R.H.; Pereyra, M.G.; De Martino, M.; Proietti, C.J.; Yankilevich, P.; et al. MiR-16 mediates trastuzumab and lapatinib response in ErbB-2-positive breast and gastric cancer via its novel targets CCNJ and FUBP1. *Oncogene* **2016**, *35*, 6189–6202. [CrossRef]
33. Xia, L.; Zhang, D.; Du, R.; Pan, Y.; Zhao, L.; Sun, S.; Hong, L.; Liu, J.; Fan, D. miR-15b and miR-16 modulate multidrug resistance by targeting BCL2 in human gastric cancer cells. *Int. J. Cancer* **2008**, *123*, 372–379. [CrossRef]
34. Chatterjee, A.; Chattopadhyay, D.; Chakrabarti, G. MiR-16 targets Bcl-2 in paclitaxel-resistant lung cancer cells and overexpression of miR-16 along with miR-17 causes unprecedented sensitivity by simultaneously modulating autophagy and apoptosis. *Cell. Signal.* **2015**, *27*, 189–203. [CrossRef]
35. Liu, Y.; Gu, S.; Li, H.; Wang, J.; Wei, C.; Liu, Q. SNHG16 promotes osteosarcoma progression and enhances cisplatin resistance by sponging miR-16 to upregulate ATG4B expression. *Biochem. Biophys. Res. Commun.* **2019**, *518*, 127–133. [CrossRef]
36. Fennell, D. miR-16: Expanding the range of molecular targets in mesothelioma. *Lancet Oncol.* **2017**, *18*, 1296–1297. [CrossRef]
37. Chen, Y.; Tsai, Y.H.; Tseng, B.J.; Pan, H.Y.; Tseng, S.H. Suppression of miR-19b enhanced the cytotoxic effects of mTOR inhibitors in human neuroblastoma cells. *J. Pediatr. Surg.* **2016**, *51*, 1818–1825. [CrossRef]
38. Thorne, J.L.; Battaglia, S.; Baxter, D.E.; Hayes, J.L.; Hutchinson, S.A.; Jana, S.; Millican-Slater, R.A.; Smith, L.; Teske, M.C.; Wastall, L.M.; et al. MiR-19b non-canonical binding is directed by HuR and confers chemosensitivity through regulation of P-glycoprotein in breast cancer. *Biochim. Biophys. Acta Gene Regul. Mech.* **2018**, *1861*, 996–1006. [CrossRef]
39. Jiang, T.; Ye, L.; Han, Z.; Liu, Y.; Yang, Y.; Peng, Z.; Fan, J. miR-19b-3p promotes colon cancer proliferation and oxaliplatin-based chemoresistance by targeting SMAD4: Validation by bioinformatics and experimental analyses. *J. Exp. Clin. Cancer Res.* **2017**, *36*, 131. [CrossRef] [PubMed]
40. Bouvy, C.; Wannez, A.; Laloy, J.; Chatelain, C.; Dogné, J.M. Transfer of multidrug resistance among acute myeloid leukemia cells via extracellular vesicles and their microRNA cargo. *Leuk. Res.* **2017**, *62*, 70–76. [CrossRef] [PubMed]
41. Wang, B.; Lu, F.Y.; Shi, R.H.; Feng, Y.D.; Zhao, X.D.; Lu, Z.P.; Xiao, L.; Zhou, G.Q.; Qiu, J.M.; Cheng, C.E. MiR-26b regulates 5-FU-resistance in human colorectal cancer via down-regulation of Pgp. *Am. J. Cancer Res.* **2018**, *8*, 2518–2527.
42. Zhao, B.; Zhang, J.; Chen, X.; Xu, H.; Huang, B. Mir-26b inhibits growth and resistance to paclitaxel chemotherapy by silencing the CDC6 gene in gastric cancer. *Arch. Med. Sci.* **2019**, *15*, 498–503. [CrossRef]

43. Tian, L.; Zhang, J.; Ren, X.; Liu, X.; Gao, W.; Zhang, C.; Sun, Y.; Liu, M. Overexpression of miR-26b decreases the cisplatin-esistance in laryngeal cancer by targeting ATF2. *Oncotarget* **2017**, *8*, 79023–79033. [CrossRef]
44. Jin, F.; Wang, Y.; Li, M.; Zhu, Y.; Liang, H.; Wang, C.; Wang, F.; Zhang, C.Y.; Zen, K.; Li, L. MiR-26 enhances chemosensitivity and promotes apoptosis of hepatocellular carcinoma cells through inhibiting autophagy. *Cell Death Dis.* **2017**, *8*, e2540. [CrossRef]
45. Zhao, N.; Wang, R.; Zhou, L.; Zhu, Y.; Gong, J.; Zhuang, S.M. MicroRNA-26b suppresses the NF-κB signaling and enhances the chemosensitivity of hepatocellular carcinoma cells by targeting TAK1 and TAB3. *Mol. Cancer* **2014**, *13*, 35. [CrossRef]
46. Wang, L.; Su, J.; Zhao, Z.; Hou, Y.; Yin, X.; Zheng, N.; Zhou, X.; Yan, J.; Xia, J.; Wang, Z. MiR-26b reverses temozolomide resistance via targeting Wee1 in glioma cells. *Cell Cycle* **2017**, *16*, 1954–1964. [CrossRef] [PubMed]
47. Lee, J.J.; Drakaki, A.; Iliopoulos, D.; Struhl, K. MiR-27b targets PPARγ to inhibit growth, tumor progression and the inflammatory response in neuroblastoma cells. *Oncogene* **2012**, *31*, 3818–3825. [CrossRef]
48. Zhang, J.; Hua, X.; Qi, N.; Han, G.; Yu, J.; Yu, Y.; Wei, X.; Li, H.; Chen, X.; Leng, C.; et al. MiR-27b suppresses epithelial-mesenchymal transition and chemoresistance in lung cancer by targeting Snail1. *Life Sci.* **2020**, *254*, 117238. [CrossRef]
49. Chen, D.; Si, W.; Shen, J.; Du, C.; Lou, W.; Bao, C.; Zheng, H.; Pan, J.; Zhong, G.; Xu, L.; et al. miR-27b-3p inhibits proliferation and potentially reverses multi-chemoresistance by targeting CBLB/GRB2 in breast cancer cells. *Cell Death Dis.* **2018**, *9*, 188. [CrossRef]
50. Shang, Y.; Feng, B.; Zhou, L.; Ren, G.; Zhang, Z.; Fan, X.; Sun, Y.; Luo, G.; Liang, J.; Wu, K.; et al. The miR27b-CCNG1-P53-miR-508-5p axis regulates multidrug resistance of gastric cancer. *Oncotarget* **2016**, *7*, 538–549. [CrossRef]
51. Hu, Z.; Cai, M.; Zhang, Y.; Tao, L.; Guo, R. miR-29c-3p inhibits autophagy and cisplatin resistance in ovarian cancer by regulating FOXP1/ATG14 pathway. *Cell Cycle* **2020**, *19*, 193–206. [CrossRef] [PubMed]
52. Li, L.; Shou, H.; Wang, Q.; Liu, S. Investigation of the potential theranostic role of KDM5B/miR-29c signaling axis in paclitaxel resistant endometrial carcinoma. *Gene* **2019**, *694*, 76–82. [CrossRef] [PubMed]
53. Wang, L.; Yu, T.; Li, W.; Li, M.; Zuo, Q.; Zou, Q.; Xiao, B. The miR-29c-KIAA1199 axis regulates gastric cancer migration by binding with WBP11 and PTP4A3. *Oncogene* **2019**, *38*, 3134–3150. [CrossRef] [PubMed]
54. Sun, D.M.; Tang, B.F.; Li, Z.X.; Guo, H.B.; Cheng, J.L.; Song, P.P.; Zhao, X. MiR-29c reduces the cisplatin resistance of non-small cell lung cancer cells by negatively regulating the PI3K/Akt pathway. *Sci. Rep.* **2018**, *8*, 8007. [CrossRef] [PubMed]
55. Xiao, S.; Yang, Z.; Qiu, X.; Lv, R.; Liu, J.; Wu, M.; Liao, Y.; Liu, Q. miR-29c contribute to glioma cells temozolomide sensitivity by targeting O6-methylguanine-DNA methyltransferases indirectely. *Oncotarget* **2016**, *7*, 50229–50238. [CrossRef] [PubMed]
56. Wang, Y.; Li, Y.; Sun, J.; Wang, Q.; Sun, C.; Yan, Y.; Yu, L.; Cheng, D.; An, T.; Shi, C.; et al. Tumor-suppressive effects of miR-29c on gliomas. *Neuroreport* **2013**, *24*, 637–645. [CrossRef] [PubMed]
57. Tang, L.J.; Sun, G.K.; Zhang, T.J.; Wu, D.H.; Zhou, J.D.; Ma, B.B.; Xu, Z.J.; Wen, X.M.; Chen, Q.; Yao, D.M.; et al. Down-regulation of miR-29c is a prognostic biomarker in acute myeloid leukemia and can reduce the sensitivity of leukemic cells to decitabine. *Cancer Cell Int.* **2019**, *19*, 177. [CrossRef]
58. Mraz, M.; Malinova, K.; Kotaskova, J.; Pavlova, S.; Tichy, B.; Malcikova, J.; Stano Kozubik, K.; Smardova, J.; Brychtova, Y.; Doubek, M.; et al. miR-34a, miR-29c and miR-17-5p are downregulated in CLL patients with TP53 abnormalities. *Leukemia* **2009**, *23*, 1159–1163. [CrossRef]
59. Ye, S.; Sun, B.; Wu, W.; Yu, C.; Tian, T.; Lian, Z.; Liang, Q.; Zhou, Y. LINC01123 facilitates proliferation, invasion and chemoresistance of colon cancer cells. *Biosci. Rep.* **2020**, *40*, BSR20194062. [CrossRef] [PubMed]
60. Zheng, H.; Wang, J.J.; Yang, X.R.; Yu, Y.L. Upregulation of miR-34c after silencing E2F transcription factor 1 inhibits paclitaxel combined with cisplatin resistance in gastric cancer cells. *World J. Gastroenterol.* **2020**, *26*, 499–513. [CrossRef]
61. Wu, H.; Huang, M.; Lu, M.; Zhu, W.; Shu, Y.; Cao, P.; Liu, P. Regulation of microtubule-associated protein tau (MAPT) by miR-34c-5p determines the chemosensitivity of gastric cancer to paclitaxel. *Cancer Chemother. Pharmacol.* **2013**, *71*, 1159–1171. [CrossRef]
62. Xiao, S.; Li, Y.; Pan, Q.; Ye, M.; He, S.; Tian, Q.; Xue, M. MiR-34c/SOX9 axis regulates the chemoresistance of ovarian cancer cell to cisplatin-based chemotherapy. *J. Cell Biochem.* **2019**, *120*, 2940–2953. [CrossRef]
63. Tung, S.L.; Huang, W.C.; Hsu, F.C.; Yang, Z.P.; Jang, T.H.; Chang, J.W.; Chuang, C.M.; Lai, C.R.; Wang, L.H. miRNA-34c-5p inhibits amphiregulin-induced ovarian cancer stemness and drug resistance via downregulation of the AREG-EGFR-ERK pathway. *Oncogenesis* **2017**, *6*, e326. [CrossRef]
64. Xu, M.; Jin, H.; Xu, C.X.; Bi, W.Z.; Wang, Y. MiR-34c inhibits osteosarcoma metastasis and chemoresistance. *Med. Oncol.* **2014**, *31*, 972. [CrossRef]
65. Liu, C.; Hou, J.; Shan, F.; Wang, L.; Lu, H.; Ren, T. Long Non-Coding RNA CRNDE Promotes Colorectal Carcinoma Cell Progression and Paclitaxel Resistance by Regulating miR-126-5p/ATAD2 Axis. *Onco Targets Ther.* **2020**, *13*, 4931–4942. [CrossRef]
66. Fu, R.; Tong, J.S. miR-126 reduces trastuzumab resistance by targeting PIK3R2 and regulating AKT/mTOR pathway in breast cancer cells. *J. Cell. Mol. Med.* **2020**, *24*, 7600–7608. [CrossRef] [PubMed]
67. Liu, W.; Chen, H.; Wong, N.; Haynes, W.; Baker, C.M.; Wang, X. Pseudohypoxia induced by miR-126 deactivation promotes migration and therapeutic resistance in renal cell carcinoma. *Cancer Lett.* **2017**, *394*, 65–75. [CrossRef] [PubMed]
68. Murray, M.J.; Raby, K.L.; Saini, H.K.; Bailey, S.; Wool, S.V.; Tunnacliffe, J.M.; Enright, A.J.; Nicholson, J.C.; Coleman, N. Solid tumors of childhood display specific serum microRNA profiles. *Cancer Epidemiol. Biomark. Prev.* **2015**, *24*, 350–360. [CrossRef]
69. Wei, J.S.; Johansson, P.; Chen, Q.R.; Song, Y.K.; Durinck, S.; Wen, X.; Cheuk, A.T.; Smith, M.A.; Houghton, P.; Morton, C.; et al. microRNA profiling identifies cancer-specific and prognostic signatures in pediatric malignancies. *Clin. Cancer Res.* **2009**, *15*, 5560–5568. [CrossRef]

70. Zeka, F.; Decock, A.; Van Goethem, A.; Vanderheyden, K.; Demuynck, F.; Lammens, T.; Helsmoortel, H.H.; Vermeulen, J.; Noguera, R.; Berbegall, A.P.; et al. Circulating microRNA biomarkers for metastatic disease in neuroblastoma patients. *JCI Insight* **2018**, *3*, e97021. [CrossRef]
71. Su, Y.K.; Lin, J.W.; Shih, J.W.; Chuang, H.Y.; Fong, I.H.; Yeh, C.T.; Lin, C.M. Targeting BC200/miR218-5p Signaling Axis for Overcoming Temozolomide Resistance and Suppressing Glioma Stemness. *Cells* **2020**, *9*, 1859. [CrossRef] [PubMed]
72. Liu, T.; Zhang, X.; Du, L.; Wang, Y.; Liu, X.; Tian, H.; Wang, L.; Li, P.; Zhao, Y.; Duan, W.; et al. Exosome-transmitted miR-128-3p increase chemosensitivity of oxaliplatin-resistant colorectal cancer. *Mol. Cancer* **2019**, *18*, 43. [CrossRef]
73. Wang, H.; Zhan, M.; Xu, S.W.; Chen, W.; Long, M.M.; Shi, Y.H.; Liu, Q.; Mohan, M.; Wang, J. miR-218-5p restores sensitivity to gemcitabine through PRKCE/MDR1 axis in gallbladder cancer. *Cell Death Dis.* **2017**, *8*, e2770. [CrossRef]
74. Li, P.; Yang, X.; Cheng, Y.; Zhang, X.; Yang, C.; Deng, X.; Li, P.; Tao, J.; Yang, H.; Wei, J.; et al. MicroRNA-218 Increases the Sensitivity of Bladder Cancer to Cisplatin by Targeting Glut1. *Cell Physiol. Biochem.* **2017**, *41*, 921–932. [CrossRef]
75. Zarogoulidis, P.; Petanidis, S.; Kioseoglou, E.; Domvri, K.; Anestakis, D.; Zarogoulidis, K. MiR-205 and miR-218 expression is associated with carboplatin chemoresistance and regulation of apoptosis via Mcl-1 and Survivin in lung cancer cells. *Cell. Signal.* **2015**, *27*, 1576–1588. [CrossRef]
76. Zeng, F.; Wang, Q.; Wang, S.; Liang, S.; Huang, W.; Guo, Y.; Peng, J.; Li, M.; Zhu, W.; Guo, L. Linc00173 promotes chemoresistance and progression of small cell lung cancer by sponging miR-218 to regulate Etk expression. *Oncogene* **2020**, *39*, 293–307. [CrossRef]
77. Chen, X.; Pan, M.; Han, L.; Lu, H.; Hao, X.; Dong, Q. miR-338-3p suppresses neuroblastoma proliferation, invasion and migration through targeting PREX2a. *FEBS Lett.* **2013**, *587*, 3729–3737. [CrossRef] [PubMed]
78. Xu, Z.; Sun, Y.; Wang, D.; Sun, H.; Liu, X. SNHG16 promotes tumorigenesis and cisplatin resistance by regulating miR-338-3p/PLK4 pathway in neuroblastoma cells. *Cancer Cell Int.* **2020**, *20*, 236. [CrossRef] [PubMed]
79. Han, L.; Cui, D.; Li, B.; Xu, W.W.; Lam, A.K.Y.; Chan, K.T.; Zhu, Y.; Lee, N.P.Y.; Law, S.Y.K.; Guan, X.Y.; et al. MicroRNA-338-5p reverses chemoresistance and inhibits invasion of esophageal squamous cell carcinoma cells by targeting Id-1. *Cancer Sci.* **2019**, *110*, 3677–3688. [CrossRef] [PubMed]
80. Creevey, L.; Ryan, J.; Harvey, H.; Bray, I.M.; Meehan, M.; Khan, A.R.; Stallings, R.L. MicroRNA-497 increases apoptosis in MYCN amplified neuroblastoma cells by targeting the key cell cycle regulator WEE1. *Mol. Cancer* **2013**, *12*, 23. [CrossRef]
81. Wang, L.; Ji, X.B.; Wang, L.H.; Qiu, J.G.; Zhou, F.M.; Liu, W.J.; Wan, D.D.; Lin, M.C.; Liu, L.Z.; Zhang, J.Y.; et al. Regulation of MicroRNA-497-Targeting AKT2 Influences Tumor Growth and Chemoresistance to Cisplatin in Lung Cancer. *Front. Cell Dev. Biol.* **2020**, *8*, 840. [CrossRef]
82. Wang, L.; Jiang, C.F.; Li, D.M.; Ge, X.; Shi, Z.M.; Li, C.Y.; Liu, X.; Yin, Y.; Zhen, L.; Liu, L.Z.; et al. MicroRNA-497 inhibits tumor growth and increases chemosensitivity to 5-fluorouracil treatment by targeting KSR1. *Oncotarget* **2016**, *7*, 2660–2671. [CrossRef]
83. Xu, S.; Fu, G.B.; Tao, Z.; Yang, J.O.; Kong, F.; Jiang, B.H.; Wan, X.; Chen, K. MiR-497 decreases cisplatin resistance in ovarian cancer cells by targeting mTOR/P70S6K1. *Oncotarget* **2015**, *6*, 26457–26471. [CrossRef]
84. Xu, J.; Wang, T.; Cao, Z.; Huang, H.; Li, J.; Liu, W.; Liu, S.; You, L.; Zhou, L.; Zhang, T.; et al. MiR-497 downregulation contributes to the malignancy of pancreatic cancer and associates with a poor prognosis. *Oncotarget* **2014**, *5*, 6983–6993. [CrossRef] [PubMed]
85. Hoareau-Aveilla, C.; Quelen, C.; Congras, A.; Caillet, N.; Labourdette, D.; Dozier, C.; Brousset, P.; Lamant, L.; Meggetto, F. miR-497 suppresses cycle progression through an axis involving CDK6 in ALK-positive cells. *Haematologica* **2019**, *104*, 347–359. [CrossRef] [PubMed]
86. Domingo-Fernandez, R.; Watters, K.; Piskareva, O.; Stallings, R.L.; Bray, I. The role of genetic and epigenetic alterations in neuroblastoma disease pathogenesis. *Pediatr. Surg. Int.* **2013**, *29*, 101–119. [CrossRef]
87. Bedrnicek, J.; Vicha, A.; Jarosova, M.; Holzerova, M.; Cinatl, J., Jr.; Michaelis, M.; Cinatl, J.; Eckschlager, T. Characterization of drug-resistant neuroblastoma cell lines by comparative genomic hybridization. *Neoplasma* **2005**, *52*, 415–419. [PubMed]
88. Wang, L.; Yang, G.; Zhao, D.; Wang, J.; Bai, Y.; Peng, Q.; Wang, H.; Fang, R.; Chen, G.; Wang, Z.; et al. CD103-positive CSC exosome promotes EMT of clear cell renal cell carcinoma: Role of remote MiR-19b-3p. *Mol. Cancer* **2019**, *18*, 86. [CrossRef] [PubMed]
89. Peng, P.; Chen, T.; Wang, Q.; Zhang, Y.; Zheng, F.; Huang, S.; Tang, Y.; Yang, C.; Ding, W.; Ren, D.; et al. Decreased miR-218-5p Levels as a Serum Biomarker in Bone Metastasis of Prostate Cancer. *Oncol. Res. Treat.* **2019**, *42*, 165–185. [CrossRef]
90. Ahmadinejad, F.; Mowla, S.J.; Honardoost, M.A.; Arjenaki, M.G.; Moazeni-Bistgani, M.; Kheiri, S.; Teimori, H. Lower expression of miR-218 in human breast cancer is associated with lymph node metastases, higher grades, and poorer prognosis. *Tumour Biol.* **2017**, *39*. [CrossRef]
91. Deng, M.; Zeng, C.; Lu, X.; He, X.; Zhang, R.; Qiu, Q.; Zheng, G.; Jia, X.; Liu, H.; He, Z. miR-218 suppresses gastric cancer cell cycle progression through the CDK6/Cyclin D1/E2F1 axis in a feedback loop. *Cancer Lett.* **2017**, *403*, 175–185. [CrossRef]
92. Jiang, Z.; Song, Q.; Zeng, R.; Li, J.; Li, J.; Lin, X.; Chen, X.; Zhang, J.; Zheng, Y. MicroRNA-218 inhibits EMT, migration and invasion by targeting SFMBT1 and DCUN1D1 in cervical cancer. *Oncotarget* **2016**, *7*, 45622–45636. [CrossRef]
93. Chiu, K.L.; Kuo, T.T.; Kuok, Q.Y.; Lin, Y.S.; Hua, C.H.; Lin, C.Y.; Su, P.Y.; Lai, L.C.; Sher, Y.P. ADAM9 enhances CDCP1 protein expression by suppressing miR-218 for lung tumor metastasis. *Sci. Rep.* **2015**, *5*, 16426. [CrossRef]

94. Marengo, B.; Pulliero, A.; Izzotti, A.; Domenicotti, C. miRNA Regulation of Glutathione Homeostasis in Cancer Initiation, Progression and Therapy Resistance. *Microrna* **2020**, *9*, 187–197. [CrossRef] [PubMed]
95. Stigliani, S.; Scaruffi, P.; Lagazio, C.; Persico, L.; Carlini, B.; Varesio, L.; Morandi, F.; Morini, M.; Gigliotti, A.R.; Esposito, M.R.; et al. Deregulation of focal adhesion pathway mediated by miR-659-3p is implicated in bone marrow infiltration of stage M neuroblastoma patients. *Oncotarget* **2015**, *6*, 13295–13308. [CrossRef] [PubMed]